

Cover Page



Universiteit Leiden



The handle <http://hdl.handle.net/1887/25979> holds various files of this Leiden University dissertation

Author: Boon, Mariëtte

Title: Turning up the heat : role of brown adipose tissue in metabolic disease

Issue Date: 2014-06-12

CENTRAL ROLE FOR BROWN ADIPOSE TISSUE IN DYSLIPIDEMIA AND ATHEROSCLEROSIS DEVELOPMENT

MARIËTTE R. BOON
JIMMY F.P. BERBÉE*
P. PADMINI S.J. KHEDOE*
ALEXANDER BARTELT*
CHRISTIAN SCHLEIN
ANNA WORTHMANN
CLARA WEIGELT
CAROLINE JUNG
SANDER KOOIJMAN
NADIA VAZIRPANAH
LINDA P.J. BROUWERS
PHILIP L.S.M. GORDTS
JEFFREY D. ESKO
PIETER S. HIEMSTRA
LOUIS M. HAVEKES
LUDGER SCHEJA
JOERG HEEREN
PATRICK C.N. RENSEN



* These authors contributed equally to this work

Submitted.

ABBREVIATIONS

ApoE	Apolipoprotein E
β 3-AR	β 3-adrenergic receptor
BAT	Brown adipose tissue
CB1R	Cannabinoid 1 receptor
CVD	Cardiovascular diseases
E3L.CETP	APOE*3-Leiden.cholesteryl ester transfer protein
EE	Energy expenditure
FA	Fatty acids
FGF21	Fibroblast growth factor 21
FPLC	Fast performance liquid chromatography
PEG	Polyethylene glycol
HE	Hematoxylin-eosin
iBAT	interscapular BAT
LDLR	Low-density lipoprotein receptor
PCSK9	Proprotein convertase subtilisin/kexin type 9
SQRT	Square root
TC	Total cholesterol
TG	Triglycerides
TO	Triolein
(V)LDL-C	(Very-)low-density lipoprotein-cholesterol
WAT	White adipose tissue
WTD	Western-type diet
UCP1	Uncoupling protein-1

ABSTRACT

Brown adipose tissue (BAT) combusts high amounts of fatty acids into heat, thereby lowering plasma triglyceride levels and reducing obesity. However, the precise role of BAT in plasma cholesterol metabolism and atherosclerosis development remains unclear. Here we show that BAT activation by the β_3 -adrenergic receptor agonist CL316243 in dyslipidemic *APOE*3-Leiden.CETP* mice, a well-established model for human-like lipoprotein metabolism, increases energy expenditure, lowers body fat and plasma triglyceride levels, and attenuates plasma cholesterol levels and the development of atherosclerosis. Mechanistically, we show that BAT activation enhanced the selective uptake of fatty acids from glycerol tri[3 H]oleate-labeled VLDL-like emulsion particles into BAT. Importantly, the cholesterol and atherosclerosis lowering effects of BAT activation were dependent on a functional hepatic apoE-LDLR clearance pathway, as BAT activation in *ApoE*^{-/-} and *Ldlr*^{-/-} mice, while lowering triglyceride levels, did not attenuate hypercholesterolemia and atherosclerosis. We demonstrate that activation of BAT is a powerful therapeutic tool to improve dyslipidemia and protect from atherosclerosis.

INTRODUCTION

Cardiovascular diseases (CVD) are the leading cause of morbidity and mortality in the Western world, and are mainly caused by atherosclerosis for which dyslipidemia is a main risk factor. As current treatment strategies of atherogenic dyslipidemia prevent only 30% of all cardiovascular events (1), novel treatment strategies are highly warranted.

Brown adipose tissue (BAT) is a highly active metabolic tissue being present and active in adults (2,3). Brown adipocytes are mainly present in fat pads, but also lie scattered in certain white adipose tissue (WAT) depots. The development of these so-called peripheral, inducible brown adipocytes or 'beige cells' can be stimulated by prolonged cold exposure or pharmacological adrenergic stimulation, a process called 'browning' (4,5). Both brown and beige adipocytes are characterized by a large number of mitochondria and numerous small lipid droplets and both cell types are functionally thermogenic (6). Physiologically, BAT is activated by cold exposure via sympathetic neurons that release noradrenalin (7). The noradrenalin-stimulated activation of brown adipocytes can be pharmacologically mimicked by selective β_3 -adrenergic receptor (β_3 -AR) treatment (8,9). Activation of the β_3 -AR rapidly induces intracellular lipolysis of TG from lipid droplets, releasing fatty acids (FA). FA are directed towards mitochondria where they either allosterically activate the uncoupling protein-1 (UCP1) in the inner membrane of the mitochondrion (10), or undergo oxidation. The intracellular TG stores of the brown adipocyte are replenished mainly by uptake of FA derived from TG-rich lipoproteins in the plasma (11).

The magnitude of the plasma TG clearance capacity of BAT became clear only recently. We showed that activation of BAT in mice via cold or metformin potently reduces plasma TG levels and obesity (12,13). Therefore, activation of BAT is now considered a promising new therapeutic avenue to combat hypertriglyceridemia and obesity (14,15). However, increased turnover of plasma lipoproteins may also lead to adverse side effects when pro-atherogenic cholesterol-rich remnants that arise from TG turnover accumulate in plasma. In that vein, BAT activation by cold exposure has been described to aggravate hypercholesterolemia and atherosclerosis development in *ApoE*^{-/-} and *Ldlr*^{-/-} mice (16). We reasoned that the enhanced clearance of plasma TG upon BAT activation requires efficient clearance of cholesterol-enriched lipoprotein remnants by the liver, a pathway that is considered to be crucially dependent on a functional apoE-LDLR axis. Here, we investigate the effects of β_3 -AR-mediated BAT activation on cholesterol metabolism and atherosclerosis development in *APOE*^{*3-Leiden}.*CETP* (*E3L.CETP*), a well-established model for human-like lipoprotein metabolism that unlike *ApoE*^{-/-} and *Ldlr*^{-/-} mice responds well to the lipid-lowering and anti-atherogenic effects of statins, fibrates and niacin (17-19).

We show that pharmacological activation of BAT in *E3L.CETP* mice enhances lipolytic conversion of TG-rich lipoproteins in BAT, resulting in a pronounced reduction in plasma cholesterol and TG levels and ultimately marked attenuation of atherosclerosis development. In addition, we show that *ApoE*^{-/-} and *Ldlr*^{-/-} mice do not respond to the plasma cholesterol-lowering activity of BAT and are not protected from atherosclerosis development, underlining the importance of the apoE-LDLR axis for the anti-atherogenic potential of BAT.

RESULTS

Activation of BAT augments fatty acid combustion and uptake under atherogenic conditions

We first assessed the effect of BAT activation on energy expenditure and lipid storage in *E3L.CETP* mice fed an atherogenic Western-type diet (WTD) for 10 weeks while treated with the selective β_3 -AR agonist CL316243 (3x 20 $\mu\text{g}/\text{mouse}/\text{week}$; subcutaneous) or vehicle (PBS). β_3 -AR agonism tended to reduce body mass (up to -8%; $P=0.05$; **FIGURE 1A**) and markedly reduced total fat mass gain (up to -81%; $P<0.001$; **FIGURE 1B**), without affecting lean mass (**FIGURE 1C**). Accordingly, in the β_3 -AR agonist-treated mice the weight of the individual WAT pads was lower (ranging from -25 to -52%; $P<0.05$; **FIGURE S1A**), and the lipid droplets within white adipocytes were smaller (-48%; $P<0.001$; **FIGURES S1B-C**).

The β_3 -AR-mediated reduction in body fat gain was likely the consequence of increased adaptive thermogenesis as energy expenditure was markedly increased on the day of treatment (+17%; $P<0.001$; **FIGURE 1D**) without differences in activity levels (**FIGURE 1E**) or food intake (not shown). The increase in energy expenditure was confined to an increased fat oxidation (+67%; $P<0.001$; **FIGURE 1F**) rather than carbohydrate oxidation (**FIGURE 1G**), and consequently, β_3 -AR agonism reduced the respiratory exchange ratio (-3.5%; $P<0.001$; **FIGURE 1H**). The enhanced energy expenditure was accompanied by a marked activation of interscapular BAT (iBAT) as evidenced by reduced intracellular lipid vacuole size in iBAT (-87%; $P<0.05$; **FIGURES S2A-B**), reduced BAT pads weight (approx. -25%; **FIGURE S1A**), and increased expression of UCP1 (+43%; $P<0.01$; **FIGURES S2C-D**). In addition, β_3 -AR agonism increased browning of WAT (**FIGURES S3A-B**).

BAT activation markedly reduced plasma TG levels throughout the treatment period (-54%; $P<0.001$; **FIGURE 2A**), caused by a reduction in VLDL-TG (**FIGURE 2B**). To confirm that this reduction was caused by enhanced uptake of TG-derived FA by BAT, we determined the effect of BAT activation on the serum decay and organ uptake of glycerol tri[^3H]oleate (triolein, TO)-labeled VLDL-mimicking emulsion particles (20). Indeed, β_3 -AR agonism markedly accelerated the serum clearance of [^3H]TO (**FIGURE 2C**; $t_{1/2} = 1.7 \pm 0.2$ vs. 3.6 ± 0.8 min; $P<0.05$) by selectively increasing the uptake of [^3H]TO-derived activity by the various BAT depots (approx. +120%; $P<0.05$; **FIGURE 2D**). Interestingly, the uptake of [^3H]oleate by WAT fat depots was also increased (approx. +120%; $P<0.01$), indicating enhanced uptake by beige adipocytes within WAT. Taken together, these data show that also under atherogenic conditions β_3 -AR agonism activates BAT *E3L.CETP* mice, resulting in increased uptake and combustion of VLDL-TG-derived FA and a consequent decrease in plasma TG levels.

Activation of BAT reduces cholesterol-rich remnant lipoproteins levels

Since disturbed cholesterol metabolism rather than disturbed triglyceride metabolism is the main determinant for atherosclerosis development (21), we next investigated the effect of BAT activation on cholesterol metabolism in *E3L.CETP* mice. BAT activation consistently reduced plasma total cholesterol (TC) levels throughout the treatment period (approx. -23%; $P<0.05$; **FIGURE 2E**) which was due to a reduction of plasma (V)LDL-cholesterol ((V)LDL-C) levels (approx. -27%; $P<0.05$; **FIGURE 2F**). Lipoprotein fractionation using fast performance liquid chromatography (FPLC) confirmed the improved cholesterol profile (**FIGURE 2G**).

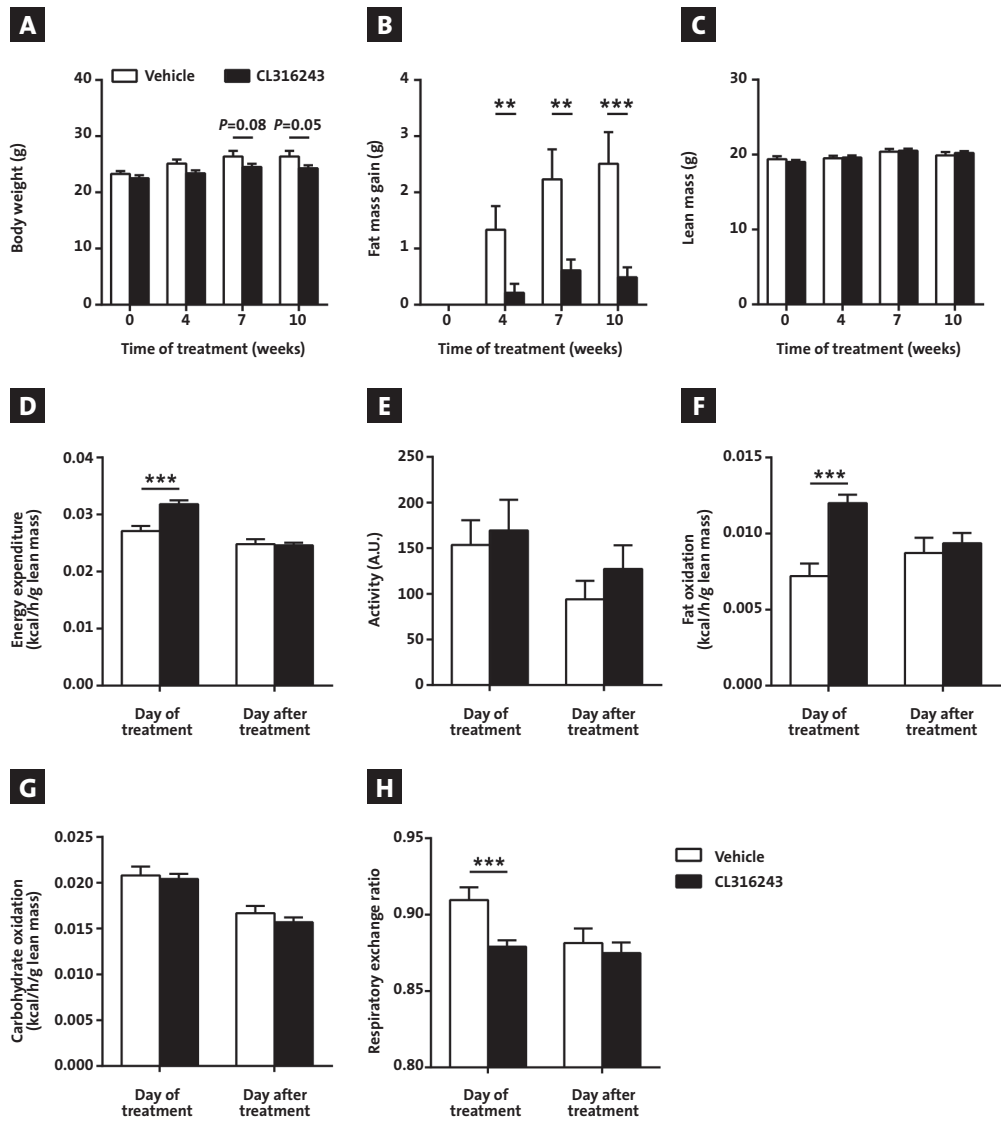


FIGURE 1 – 3-AR agonism reduces body fat mass and increases energy expenditure. Western-type diet-fed *E3L.CETP* mice were treated with the β_3 -AR agonist CL316243 or vehicle and body weight **A**, gain of total body fat mass **B** and lean mass **C** were determined at the indicated time points. During the ninth week of treatment, mice were housed in fully automated metabolic cages and energy expenditure **D**, physical activity **E**, fat oxidation **F** and carbohydrate oxidation **G** were determined. In addition, respiratory exchange ratio was determined **H**. Data are shown as the first 12 hours directly after the injection with CL316243 or vehicle ('Day of treatment') and the same 12-hours period 24 hours later ('Day after treatment').

Values are means \pm S.E.M. (n=13-19 per group). ** $P < 0.01$, *** $P < 0.001$

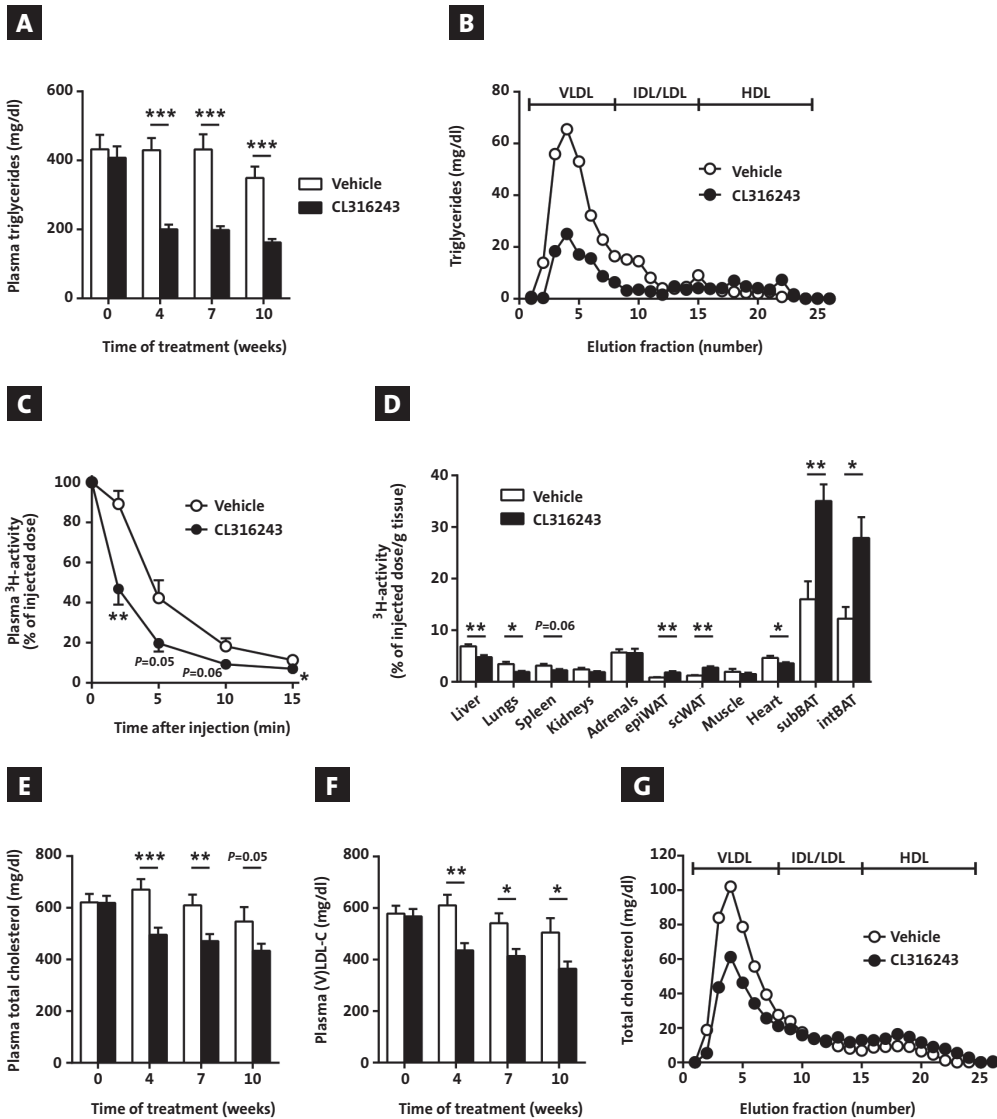
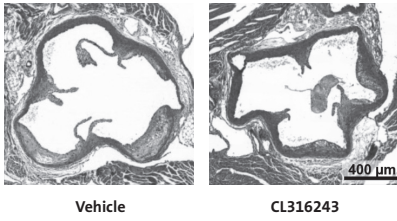
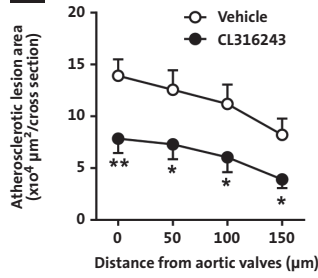
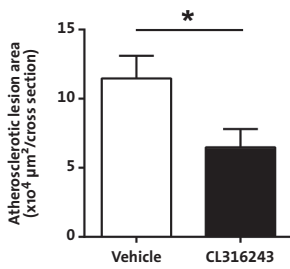
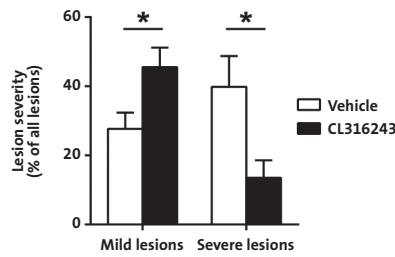


FIGURE 2 – Activation of BAT improves both TG and cholesterol metabolism. Western-type diet-fed *E3L.CETP* mice were treated with the β_3 -AR agonist CL316243 or vehicle and fasting plasma TG levels **A** were measured at the indicated time points. The distribution of TG over lipoproteins was determined after 10 weeks of treatment on pooled plasma samples per group **B**. CL316243- and vehicle-treated mice were injected with [^3H]TO-labeled VLDL-like emulsion particles and clearance from plasma **C** and organ and tissue uptake 15 min after injection **D** were determined. Fasting plasma total cholesterol **E** and (V)LDL-cholesterol ((V)LDL-C; **F**) were assessed at the indicated times during the study. The distribution of total cholesterol over lipoproteins was determined after 10 weeks of treatment on pooled plasma samples per group **G**.

Values are means \pm S.E.M. (n=13-19 per group). * $P < 0.05$, ** $P < 0.01$, *** $P < 0.001$

A**B****C****D**

9

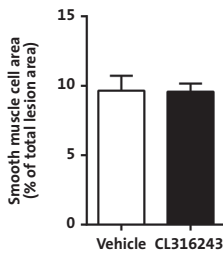
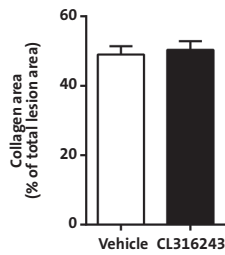
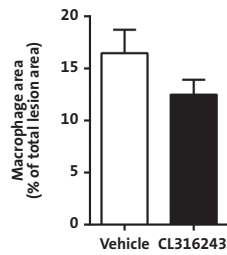
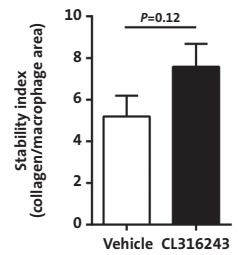
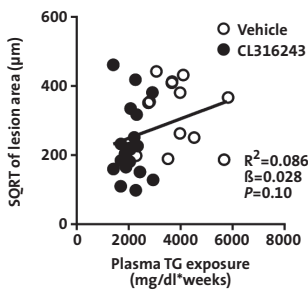
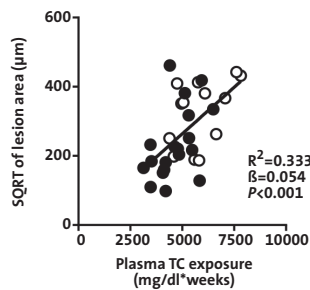
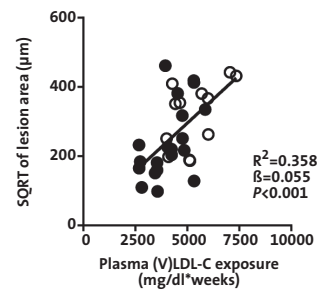
E**F****G****H****I****J****K**

FIGURE 3 – Activation of BAT reduces atherosclerotic lesion development and severity via improving the plasma cholesterol profile. Slides of the valve area of the aortic root of β_3 -AR agonist CL316243- and vehicle-treated *E3L.CETP* mice were stained with hematoxylin-phloxine-saffron and representative pictures are shown **A**. Lesion area as a function of distance was determined in four consecutive sections per mouse starting from the appearance of open aortic valve leaflets **B**. The mean atherosclerotic lesion area was determined from the four cross sections from **B** **C** and lesions were categorized according to lesion severity **D**. The smooth muscle cell **E**, collagen **F** and macrophage **G** content of the lesions were determined and the stability index (collagen/macrophage content of the lesions; **H**) was calculated. The square root (SQRT) of the atherosclerotic lesion area from **B** was plotted against the plasma total TG **I**, total cholesterol **J** and (V)LDL-cholesterol ((V)LDL-C; **K**) exposure during the 10 week treatment period. Linear regression analyses were performed.

Values are means \pm S.E.M. (n=13-19 per group). * $P < 0.05$, ** $P < 0.01$

Activation of BAT reduces atherosclerosis development by improving the plasma cholesterol profile

Next, we studied whether the decreased (V)LDL levels were accompanied by reduced atherosclerosis development. To this end, we determined atherosclerotic lesion area as well as severity and composition of the lesions in the root of the aortic arch after 10 weeks of BAT activation. Indeed, sustained BAT activation by β_3 -AR agonism markedly reduced atherosclerotic lesion area throughout the aortic root (**FIGURES 3A-B**), resulting in 43% lower mean atherosclerotic lesion area (**FIGURE 3C**). BAT activation clearly reduced the severity of the lesions, as indicated by more mild lesions (*i.e.* type I-III; +64%; $P < 0.05$) and less severe lesions (*i.e.* type IV-V; -66%; $P < 0.05$) (**FIGURE 3D**) without significantly affecting atherosclerotic lesion composition (*i.e.* collagen, vascular smooth muscle cell and macrophage content of the lesions; **FIGURES 3E-G**) or the lesion stability index (*i.e.* ratio collagen/macrophage area; **FIGURE 3H**).

To evaluate the contribution of TG versus TC lowering to the reduction in atherosclerosis, univariate regression analyses were performed. To linearize data for analysis, the atherosclerotic lesion area was square root (SQRT)-transformed (19) and plotted against the exposure (*i.e.* AUC of plasma lipid for the complete treatment period) of TG, and TC. The SQRT of the lesion area did not correlate with plasma TG exposure ($\beta = 0.028$; $R^2 = 0.086$; $P = 0.10$; **FIGURE 3I**), but did correlate with plasma TC exposure ($\beta = 0.054$; $R^2 = 0.333$; $P < 0.001$; **FIGURE 3J**). Additional univariate regression analyses showed that the (V)LDL-C exposure specifically predicts the SQRT of the lesion area ($\beta = 0.055$; $R^2 = 0.358$; $P < 0.001$; **FIGURE 3K**). These analyses thus strongly indicate that a reduction in plasma (V)LDL-C is the main contributor to the anti-atherogenic effect of β_3 -AR-mediated activation of BAT.

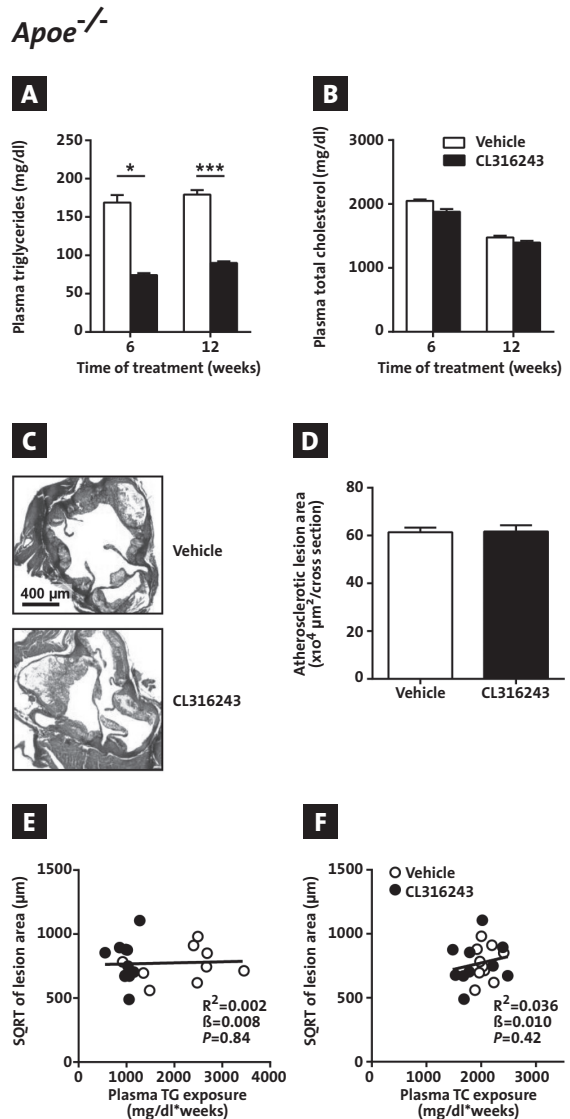
The anti-atherogenic potential of BAT activation crucially depends on functional hepatic lipoprotein clearance

As BAT activation by cold in *Apoe*^{-/-} and *Ldlr*^{-/-} mice has been described to aggravate atherosclerosis development (16), we evaluated the role of apoE, the main clearance ligand for TG-rich lipoprotein remnants, in the (V)LDL-C-reducing effect of BAT activation. In order to control for increases in food intake as described in these mouse models during cold adaption (16), as well as to match dietary cholesterol intake we studied the effect of β_3 -AR-mediated BAT activation in WTD-pair-fed *Apoe*^{-/-} mice. Similar as in *E3L.CETP* mice, activation of BAT

reduced body weight, WAT pad size and plasma TG levels (FIGURES 4A and 54A-C). However, activation of BAT did neither reduce plasma TC and (V)LDL-C levels (FIGURES 4B and 54D) nor did it reduce atherosclerosis development (FIGURES 4C-D) or alter plaque composition (data not shown) in *ApoE*^{-/-} mice. Accordingly, the SQRT of the lesion area did not correlate with either total plasma TG exposure or plasma TC exposure during the study (FIGURES 4E-F).

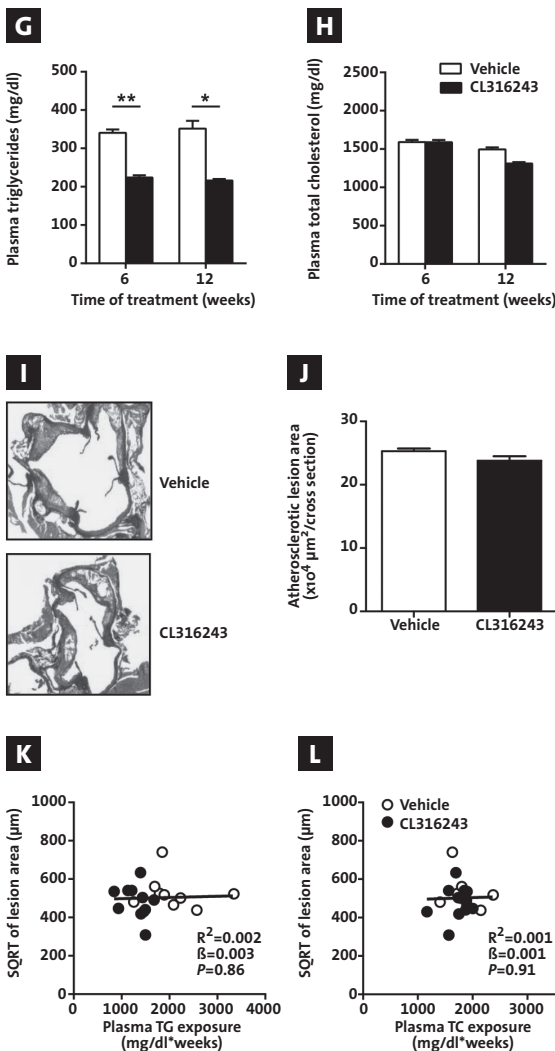
As the (V)LDL-C-reducing effect of BAT activation thus crucially depends on apoE-mediated clearance, we next investigated the role of the LDLR, the main hepatic clearance receptor for apoE-containing lipoprotein remnants. Similar as in *E3L.CETP* mice, activation of BAT

FIGURE 4 - Activation of BAT in *ApoE*^{-/-} and *Ldlr*^{-/-} mice reduces plasma TG, but not TC and atherosclerosis. Western-type diet-fed *ApoE*^{-/-} mice were treated with the β_3 -AR agonist CL316243 or vehicle and fasting plasma TG **A** and total cholesterol **B** levels were measured at the indicated time points. Slides of the valve area of the aortic root of CL316243- or vehicle-treated *ApoE*^{-/-} mice were stained with hematoxylin-phloxine-saffron (HPS) and representative pictures are shown **C**. Mean atherosclerotic lesion area was determined from four consecutive cross sections per mouse starting from the appearance of open aortic valve leaflets **D**. The square root (SQRT) of the atherosclerotic lesion area from D in *ApoE*^{-/-} mice was plotted against the plasma total TG **E** and total cholesterol **F** exposure during the 12-week treatment period. Linear regression analyses were performed.



reduced body weight, WAT pad size and plasma TG levels in WTD-pair-fed *Ldlr*^{-/-} mice (**FIGURES 4G** and **55A-C**). However, activation of BAT in *Ldlr*^{-/-} mice did neither reduce plasma TC and (V) LDL-C levels (**FIGURES 4H** and **55D**), nor reduce atherosclerosis development (**FIGURES 4I-J**) or alter plaque composition (data not shown), nor did the SQRT of the lesion area correlate with the total plasma TG and TC exposure during the study (**FIGURES 4K-L**). Taken together, these findings indicate that activation of BAT reduces plasma (V)LDL-C and subsequently reduces atherosclerosis development through enhanced LDLR-mediated hepatic clearance of apoE-containing lipoprotein remnants.

Ldlr^{-/-}



Western-type diet-fed *Ldlr*^{-/-} mice were treated with the β₃-AR agonist CL316243 or vehicle and fasting plasma TG **G** and total cholesterol **H** levels were measured at the indicated time points. Slides of the valve area of the aortic root of CL316243- or vehicle-treated *Ldlr*^{-/-} mice were stained with HPS and representative pictures are shown **I**. Mean atherosclerotic lesion area was determined from four consecutive cross sections per mouse starting from the appearance of open aortic valve leaflets **J**. The square root (SQRT) of the atherosclerotic lesion area from **J** in *Ldlr*^{-/-} mice was plotted against the plasma total TG **K** and total cholesterol **L** exposure during the 12-week treatment period. Linear regression analyses were performed.

Values are means ± S.E.M. (n=8-11 per group or pool). *P<0.05, **P<0.01, ***P<0.001

DISCUSSION

Since its rediscovery in human adults in 2009 (2,3,22), BAT has been considered a promising therapeutic target for obesity and associated metabolic disorders. The anti-obesity potential of BAT has been irrefutably proven in murine studies (23,24) and shown in human studies (2,25,26). However, the effect of BAT activation on cholesterol metabolism and atherosclerosis development remained controversial if not elusive. The present study demonstrates that activation of BAT potentially improves plasma cholesterol metabolism via a mechanism involving local lipolysis of TG-rich lipoproteins in BAT followed by increased clearance of apoE-containing lipoprotein remnants via the LDLR pathway. As a result, BAT activation reduces atherosclerotic lesion size and severity.

We observed that BAT activation decreased atherosclerosis development in *E3L.CETP* mice that possess a functional apoE-LDLR clearance pathway, but not in *ApoE*^{-/-} and *Ldlr*^{-/-} mice, both of which have an abrogated apoE-LDLR clearance pathway. This indicates that a crucial event in the anti-atherogenic property of BAT is the concomitant ability of the liver to clear apoE-enriched lipoprotein remnants, generated by BAT-mediated lipolysis of TG-rich lipoproteins, via the LDLR. *E3L.CETP* mice express a naturally occurring mutant form of human apoE3 that slows down remnant clearance, but does not abrogate the interaction with the LDLR (27). This results in an attenuated hepatic remnant clearance that is sufficient to induce dyslipidemia and atherosclerosis when feeding a WTD, but, importantly, the hepatic remnant clearance route is still functional and can be modulated. Accordingly, *E3L.CETP* mice respond to cholesterol-lowering drugs such as statins (18), fibrates (17) and niacin (19) in a similar manner as humans, whereas *ApoE*^{-/-} and *Ldlr*^{-/-} mice do not. According to this view, it is not surprising that Dong *et al.* (16) recently observed that BAT activation by cold in *ApoE*^{-/-} and *Ldlr*^{-/-} mice actually increased plasma (V)LDL-C levels and atherosclerosis. Likely, in these hyperlipidemic mouse models prolonged BAT activation results in lipoprotein remnant levels in plasma exceeding the hepatic clearance capacity.

Our work sets the foundation for future studies that may investigate the anti-atherogenic potential of BAT in humans. As the discovery that functional BAT is present and active in human adults was made only in the last decade (2,3), recent studies have focused on the physiological relevance of BAT for humans. That BAT is likely involved in energy metabolism and obesity development in humans appeared from studies that showed that BAT activity is inversely correlated to obesity (28) and that cold acclimation recruits BAT (29) and lowers fat mass (26). In addition, South Asians, who have a high susceptibility to metabolic disorders, have decreased energy expenditure associated with decreased BAT volume and activity (30). Importantly, BAT activation by means of cold acclimation also improved cholesterol metabolism in human patients with hypercholesterolemia (31), underscoring the potential of BAT activation as an anti-atherogenic treatment in humans. Future prospective studies are evidently needed to verify the anti-atherogenic properties of BAT activation in human subjects.

Though the β_3 -AR is abundantly present on rodent BAT, it is still uncertain whether this isoform also controls BAT activity in humans. Although differentiated brown adipocytes from human multipotent adipose-derived stem cells could be activated by the β_3 -AR agonist

CL316243 (32), treatment of humans with β_3 -AR agonists showed no or only minor improvement of metabolic parameters (33,34). This may be due to low bioavailability of the agonist or low β_3 -AR expression in human BAT, as plasma concentration of the agonist and reduction in fat mass and resting metabolic rate were in fact positively correlated. Alternatively, the β_1 -AR and/or β_2 -AR may be involved in human BAT function, as blockade of these receptors by propranolol decreased ^{18}F -fluorodeoxyglucose uptake by BAT as visualized by PET-CT scans (35), though the thermogenic responses remain unaffected (36). Collectively, this may suggest that ^{18}F -fluorodeoxyglucose uptake is regulated by β_1 - or β_2 -ARs, whereas mitochondrial uncoupling itself is regulated by β_3 -ARs. Future studies should thus be directed at investigating the precise role of β -ARs in human BAT function.

The long-term objective of this work is to set out novel therapeutic targets to activate BAT beyond β -AR stimulation. Promising targets include the cannabinoid 1 receptor (CB1R) on BAT (Boon and Rensen, unpublished), irisin (37) and the fibroblast growth factor FGF21 (37), which massively activate BAT and induce browning in mice, and lowers plasma cholesterol in both mice and humans (37-39).

In conclusion, our data demonstrate that activation of BAT lowers plasma cholesterol levels and protects against atherosclerosis development, a scenario that is dependent on the apoE-LDLR clearance pathway for lipoprotein remnants. Future research should focus on elucidating whether BAT activation is a valuable strategy to combat obesity and atherosclerosis in humans. We expect that BAT activation, resulting in accelerated generation of lipoprotein remnants, should preferentially be combined with strategies that increase hepatic LDLR expression, including statins and/or PCSK9 blockers, fully unraveling the therapeutic potential of BAT for atherosclerosis prevention and treatment.

EXPERIMENTAL PROCEDURES

Animals, diet and β_3 -AR agonist treatment

Female *E3L* were crossbred with mice expressing human cholesteryl ester transfer protein (CETP) under control of its natural flanking regions to generate heterozygous *E3L.CETP* mice (18). Female *E3L.CETP* mice were 10-12 weeks of age and housed under standard conditions with a 12-hours light/dark cycle, free access to food and water and 22°C room temperature. Mice were fed a Western-type diet (WTD) supplemented with 0.1% cholesterol and treated with the β_3 -AR agonist CL316243 (Tocris Bioscience Bristol, United Kingdom; 3x 20 μg /mouse/week; subcutaneous) or vehicle (PBS). Food intake and body weight as well as total body fat and lean mass by Echo-MRI were monitored during the studies. Male *Apoe*^{-/-} and *Ldlr*^{-/-} mice (Jackson Laboratory, Bar Harbor, ME) were fed a WTD supplemented with 0.2% cholesterol with or without CL316243 (0.001% w/w). As CL316243 treatment of *Apoe*^{-/-} and *Ldlr*^{-/-} mice increased food intake, these mice were pair-fed to their respective controls after onset of effect. All animal experiments were approved by the Institutional Ethics Committees on Animal Care and Experimentation.

Indirect calorimetry

Indirect calorimetry was performed in fully automatic metabolic cages (LabMaster System, TSE Systems, Bad Homburg, Germany) during the ninth week of treatment. After 1 day of acclimatization, O₂ consumption, CO₂ production and caloric intake were measured for 3 consecutive days. Carbohydrate and fat oxidation rates were calculated from O₂ consumption and CO₂ production as described previously (40). Total energy expenditure (EE) was calculated from the sum of carbohydrate and fat oxidation. Physical activity was monitored using infrared sensor frames. The first 12 h directly after injection with CL316243 or vehicle ('Day of treatment') were analysed and compared to the same 12-h period 24 h later ('Day after treatment').

In vivo serum decay and organ uptake of VLDL-like emulsion particles

VLDL-like TG-rich emulsion particles (80 nm) labeled with glycerol tri[³H]-oleate (triolein, TO) were prepared and characterized as described previously (20). After 4 weeks of treatment with the β ₃-AR agonist CL316243 mice were fasted for 4 h, and injected (t=0) via the tail vein with the emulsion particles (1.0 mg TG/mouse in 200 μ l PBS). Blood samples were taken from the tail vein at 2, 5, 10 and 15 min after injection to determine the serum decay of [³H] TO. Plasma volumes were calculated as 0.04706 x body weight (g) as described (41). After 15 min, mice were sacrificed by cervical dislocation and perfused with ice-cold heparin solution (0.1% v/v in PBS) via the heart to remove blood from the organs and tissues. Subsequently, organs and tissues were isolated, dissolved overnight at 56°C in Tissue Solubilizer (Amersham Biosciences, Rosendaal, The Netherlands), and quantified for ³H-activity. Uptake of [³H] TO-derived radioactivity by the organs and tissues was expressed per gram wet tissue weight.

Plasma parameters and lipoprotein profiles

Blood was collected from the tail vein of 4-h fasted mice into EDTA- (*E3L.CETP*) or lithium-heparin-coated tubes (*ApoE*^{-/-} and *Ldlr*^{-/-} mice). Tubes were placed on ice, centrifuged, and plasma was isolated and assayed for TG and TC using commercially available enzymatic kits from Roche Diagnostics (Mannheim, Germany). Plasma HDL-C levels were determined by precipitating apoB-containing lipoproteins from plasma by addition of 20% polyethylene glycol (PEG) in 200 mM glycine buffer with pH 10, and TC was measured in the supernatant as described above. Plasma (V)LDL-C levels were calculated by extraction of HDL-C from TC levels. The distribution of triglycerides and cholesterol over lipoproteins was determined in pooled plasma by fast performance liquid chromatography on a Superose 6 column (GE Healthcare, Piscataway, NJ).

Sacrification and Histology of BAT and WAT

At the end of the study mice were anesthetized by intraperitoneal injection of acepromazine (6.25 mg/kg; Alfasan, Woerden, The Netherlands), midazolam (0.25 mg/kg; Roche, Mijdrecht, The Netherlands) and fentanyl (0.31 mg/kg; Janssen-Cilag, Tilburg, The Netherlands), bled and killed by cervical dislocation or transcardial blood withdrawal. The blood circulation was

perfused with ice-cold heparin solution (0.1% v/v in PBS) and organs and tissues were weighed and collected for further analyses. Epididymal WAT and interscapular BAT were removed and fixated in phosphate-buffered 4% formaldehyde and embedded in paraffin. Hematoxylin-eosin (HE) staining was performed using standard protocols. Intracellular lipid droplet size in WAT and percentage of lipid-droplet-positive area in BAT were quantified using Image J software (version 1.47).

For UCP1 staining, 5 μm sections were deparaffinized in xylene, rehydrated in ethanol and treated with 3% H_2O_2 (Sigma-Aldrich, Zwijndrecht, The Netherlands) in absolute methanol for 30 min to block endogenous peroxidase activity. Sections were immersed in citrate buffer (10 mM, pH 6) and boiled for 10 min. Slides were blocked with 1.3% normal goat serum (in PBS) and incubated overnight at 4°C with rabbit monoclonal anti-UCP1 antibody (Abcam, Cambridge, United Kingdom; 1:400 in 1.3% normal goat serum). Subsequently, sections were incubated for 60 min with biotinylated goat α -rabbit secondary antibody (Vector Labs, Burlingame, CA) diluted in 1.3% normal goat serum. Immunostaining was amplified using Vector Laboratories Elite ABC kit (Vector Labs) and the immunoperoxidase complex was visualized with Nova Red (Vector Labs). Counterstaining was performed with Mayer's hematoxylin (1:4). Expression of UCP1 was quantified using Image J software (version 1.47).

Atherosclerosis quantification

Hearts were collected and fixated in phosphate-buffered 4% formaldehyde, embedded in paraffin and perpendicular to the axis of the aorta cross-sectioned (5 μm) throughout the aortic root area starting from the appearance of open aortic valve leaflets. Per mouse 4 sections with 50 μm intervals were used for atherosclerosis measurements. Sections were stained with hematoxylin-phloxine-saffron for histological analysis. Lesions were categorized for lesion severity according to the guidelines of the American Heart Association adapted for mice (42). Various types of lesions were discerned: mild lesions (types 1-3) and severe lesions (types 4-5). Lesion area was determined using Image J Software (version 1.47). Lesion composition with respect to smooth muscle cell and collagen content was determined as described previously (42). Rat monoclonal anti-MAC-3 antibody (BD Pharmingen, San Diego, CA) was used to quantify macrophage area. The stability index was calculated by dividing the collagen by the macrophage area.

Statistical analyses

Statistical analyses were assessed using the unpaired two-tailed Student's t-test. Univariate regression analyses were performed to test for significant correlations between atherosclerotic lesion area and plasma lipid exposures during the study. Multiple regression analysis was performed to predict the contribution of plasma TG and TC exposures during the study to the atherosclerotic lesion area. The square root (SQRT) of the lesion area was taken to linearize the relationship with the plasma lipid exposures. Data are presented as mean \pm S.E.M., unless indicated otherwise. A probability level (*P*) of 0.05 was considered significant. SPSS 20.0 for Windows (SPSS, Chicago, IL) was used for statistical analyses.

ACKNOWLEDGMENTS

This study is supported by ‘the Netherlands CardioVascular Research Initiative: the Dutch Heart Foundation, Dutch Federation of University Medical Centers, the Netherlands Organisation for Health Research and Development and the Royal Netherlands Academy of Sciences’ for the GENIUS project ‘Generating the best evidence-based pharmaceutical targets for atherosclerosis’ (CVON2011-19). M.R. Boon is supported by a personal grant from the Board of Directors of LUMC, P.P.S.J. Khedoe by a grant of the Lung Foundation Netherlands (grant 3.2.10.048), and P.C.N. Rensen is an Established Investigator of the Netherlands Heart Foundation (grant 2009To38). A. Bartelt was supported by a Postdoctoral Fellowship Award from the European Atherosclerosis Society (EAS) and a Research Fellowship from the German Research Foundation (DFG; BA 4925/1-1). J. Heeren is supported by a grant from the Fondation Leducq – Triglyceride Metabolism in Obesity and Cardiovascular Disease. Furthermore, the authors thank Isabel M. Mol, Lianne C.J.A. van der Wee-Pals, Trea Streefland and Chris van der Bent (Dept. of Endocrinology and Metabolic Diseases, LUMC, Leiden, The Netherlands) as well as Sandra Ehret (Dept. of Biochemistry and Molecular Cell Biology, Hamburg, Germany) for their excellent technical assistance and Dr. Jan B. van Klinken (Dept. of Human Genetics, LUMC, Leiden, The Netherlands) for help with statistical analysis. The authors would like to thank A.J. Whittle and A. Vidal-Puig for critical discussions.

REFERENCES

- 1 Jukema JW, Cannon CP, de Craen AJ, et al. The controversies of statin therapy: weighing the evidence. *J Am Coll Cardiol* 60:875-881, 2012.
- 2 van Marken Lichtenbelt WD, Vanhommel JW, Smulders NM, et al. Cold-activated brown adipose tissue in healthy men. *N Engl J Med* 360:1500-1508, 2009.
- 3 Virtanen KA, Lidell ME, Orava J, et al. Functional brown adipose tissue in healthy adults. *N Engl J Med* 360:1518-1525, 2009.
- 4 Bartelt A, Heeren J: Adipose tissue browning and metabolic health. *Nat Rev Endocrinol* 2013.
- 5 Wu J, Bostrom P, Sparks LM, et al. Beige adipocytes are a distinct type of thermogenic fat cell in mouse and human. *Cell* 150:366-376, 2012.
- 6 Shabalina IG, Petrovic N, de Jong JM, et al. UCP1 in brite/beige adipose tissue mitochondria is functionally thermogenic. *Cell Rep* 5:1196-1203, 2013.
- 7 Cannon B, Nedergaard J: Brown adipose tissue: function and physiological significance. *Physiol Rev* 84:277-359, 2004.
- 8 Lowell BB, Spiegelman BM: Towards a molecular understanding of adaptive thermogenesis. *Nature* 404:652-660, 2000.
- 9 Zhao J, Cannon B, Nedergaard J: Thermogenesis is beta3- but not beta1-adrenergically mediated in rat brown fat cells, even after cold acclimation. *Am J Physiol* 275:R2002-R2011, 1998.
- 10 Fedorenko A, Lishko PV, Kirichok Y: Mechanism of fatty-acid-dependent UCP1 uncoupling in brown fat mitochondria. *Cell* 151:400-413, 2012.
- 11 Bartelt A, Merkel M, Heeren J: A new, powerful player in lipoprotein metabolism: brown adipose tissue. *J Mol Med (Berl)* 90:887-893, 2012.
- 12 Bartelt A, Bruns OT, Reimer R, et al. Brown adipose tissue activity controls triglyceride clearance. *Nat Med* 17:200-205, 2011.
- 13 Geerling JJ, Boon MR, van der Zon GC, et al. Metformin lowers plasma triglycerides by promoting VLDL-triglyceride clearance by brown adipose tissue in mice. *Diabetes* 2013.
- 14 Bartelt A, Heeren J: The holy grail of metabolic disease: brown adipose tissue. *Curr Opin Lipidol* 23:190-195, 2012.
- 15 Harms M, Seale P: Brown and beige fat: development, function and therapeutic potential. *Nat Med* 19:1252-1263, 2013.
- 16 Dong M, Yang X, Lim S, et al. Cold exposure promotes atherosclerotic plaque growth and instability via UCP1-dependent lipolysis. *Cell Metab* 18:118-129, 2013.
- 17 Bijland S, Pieterman EJ, Maas AC, et al. Fenofibrate increases very low density lipoprotein triglyceride production despite reducing plasma triglyceride levels in APOE*3-Leiden.CETP mice. *J Biol Chem* 285:25168-25175, 2010.
- 18 De Haan W, de Vries-van der Weij, van der Hoorn JW, et al. Torcetrapib does not reduce atherosclerosis beyond atorvastatin and induces more proinflammatory lesions than atorvastatin. *Circulation* 117:2515-2522, 2008.
- 19 Kuhnast S, Louwe MC, Heemskerk MM, et al. Niacin Reduces Atherosclerosis Development in APOE*3Leiden.CETP Mice Mainly by Reducing NonHDL-Cholesterol. *PLoS One* 8:e66467, 2013.
- 20 Rensen PC, van Dijk MC, Havenaar EC, et al. Selective liver targeting of antivirals by recombinant chylomicrons--a new therapeutic approach to hepatitis B. *Nat Med* 1:221-225, 1995.
- 21 Libby P, Ridker PM, Hansson GK: Progress and challenges in translating the biology of atherosclerosis. *Nature* 473:317-325, 2011.
- 22 Cypess AM, Lehman S, Williams G, et al. Identification and importance of brown adipose tissue in adult humans. *N Engl J Med* 360:1509-1517, 2009.
- 23 Dulloo AG, Miller DS: Energy balance following sympathetic denervation of brown adipose tissue. *Can J Physiol Pharmacol* 62:235-240, 1984.
- 24 Kozak LP, Koza RA, Anunciado-Koza R: Brown fat thermogenesis and body weight regulation in mice: relevance to humans. *Int J Obes (Lond)* 34 Suppl 1:S23-S27, 2010.
- 25 Wang Q, Zhang M, Ning G, et al. Brown adipose tissue in humans is activated by elevated plasma catecholamines levels and is inversely related to central obesity. *PLoS One* 6:e21006, 2011.

- 26 Yoneshiro T, Aita S, Matsushita M, et al. Recruited brown adipose tissue as an antiobesity agent in humans. *J Clin Invest* 123:3404-3408, 2013.
- 27 van Vlijmen BJ, van den Maagdenberg AM, Gijbels MJ, et al. Diet-induced hyperlipoproteinemia and atherosclerosis in apolipoprotein E3-Leiden transgenic mice. *J Clin Invest* 93:1403-1410, 1994.
- 28 Vijgen GH, Bouvy ND, Teule GJ, et al. Brown adipose tissue in morbidly obese subjects. *PLoS One* 6:e17247, 2011.
- 29 van der Lans AA, Hoeks J, Brans B, et al. Cold acclimation recruits human brown fat and increases nonshivering thermogenesis. *J Clin Invest* 123:3395-3403, 2013.
- 30 Bakker LE, Boon MR, van der Linden RA, et al. Brown adipose tissue volume in healthy lean south Asian adults compared with white Caucasians: a prospective, case-controlled observational study. *Lancet Diabetes Endocrinol* in press: 2014.
- 31 De Lorenzo F, Mukherjee M, Kadziola Z, et al. Central cooling effects in patients with hypercholesterolaemia. *Clin Sci (Lond)* 95:213-217, 1998.
- 32 Mattsson CL, Csikasz RI, Chernogubova E, et al. beta(1)-Adrenergic receptors increase UCP1 in human MADS brown adipocytes and rescue cold-acclimated beta(3)-adrenergic receptor-knockout mice via nonshivering thermogenesis. *Am J Physiol Endocrinol Metab* 301:E1108-E1118, 2011.
- 33 Larsen TM, Toubro S, van Baak MA, et al. Effect of a 28-d treatment with L-796568, a novel beta(3)-adrenergic receptor agonist, on energy expenditure and body composition in obese men. *Am J Clin Nutr* 76:780-788, 2002.
- 34 Redman LM, de JL, Fang X, et al. Lack of an effect of a novel beta3-adrenoceptor agonist, TAK-677, on energy metabolism in obese individuals: a double-blind, placebo-controlled randomized study. *J Clin Endocrinol Metab* 92:527-531, 2007.
- 35 Parysow O, Mollerach AM, Jager V, et al. Low-dose oral propranolol could reduce brown adipose tissue F-18 FDG uptake in patients undergoing PET scans. *Clin Nucl Med* 32:351-357, 2007.
- 36 Wijers SL, Saris WH, van Marken Lichtenbelt WD: Cold-induced adaptive thermogenesis in lean and obese. *Obesity (Silver Spring)* 18:1092-1099, 2010.
- 37 Lee P, Linderman JD, Smith S, et al. Irisin and FGF21 Are Cold-Induced Endocrine Activators of Brown Fat Function in Humans. *Cell Metab* 19:302-309, 2014.
- 38 Emanuelli B, Vienberg SG, Smyth G, et al. Interplay between FGF21 and insulin action in the liver regulates metabolism. *J Clin Invest* 2014.
- 39 Gaich G, Chien JY, Fu H, et al. The effects of LY2405319, an FGF21 analog, in obese human subjects with type 2 diabetes. *Cell Metab* 18:333-340, 2013.
- 40 van Klinken JB, van den Berg SA, Havekes LM, et al. Estimation of activity related energy expenditure and resting metabolic rate in freely moving mice from indirect calorimetry data. *PLoS One* 7:e36162, 2012.
- 41 Jong MC, Rensen PC, Dahlmans VE, et al. Apolipoprotein C-III deficiency accelerates triglyceride hydrolysis by lipoprotein lipase in wild-type and apoE knockout mice. *J Lipid Res* 42:1578-1585, 2001.
- 42 Wong MC, van Diepen JA, Hu L, et al. Hepatocyte-specific IKKbeta expression aggravates atherosclerosis development in APOE*3-Leiden mice. *Atherosclerosis* 220:362-368, 2012.

SUPPLEMENTARY APPENDIX

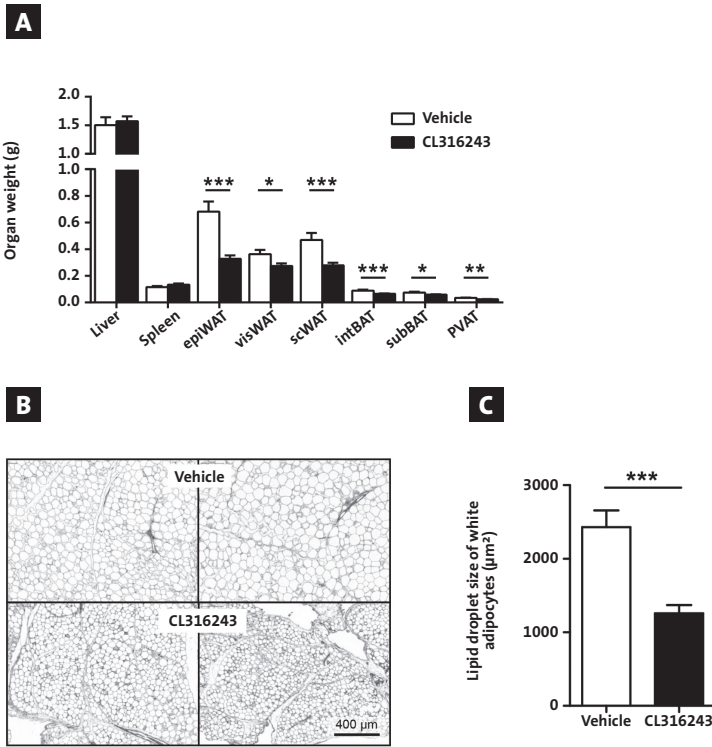


FIGURE S1 – β_3 -AR agonism reduces adiposity and lipid droplet size in white adipose tissue. *E3L.CETP* mice were fed a Western-type diet and treated with the β_3 -AR agonist CL316243 or vehicle for 10 weeks. After sacrifice at week 10, the weight of various organs was determined **A**. Epididymal white adipose tissue (epiWAT) was stained with hematoxylin-eosin (HE) and representative pictures are shown **B**. Lipid droplet size of white adipocytes was determined using Image J software **C**. visWAT, visceral WAT; scWAT, subcutaneous WAT; intBAT, interscapular brown adipose tissue; subBAT, subscapular BAT; PVAT, perivascular adipose tissue. Values are means \pm S.E.M. (panel A-B: n=13-19 per group; panel D: n=8 per group). * $P < 0.05$, ** $P < 0.01$, *** $P < 0.001$.

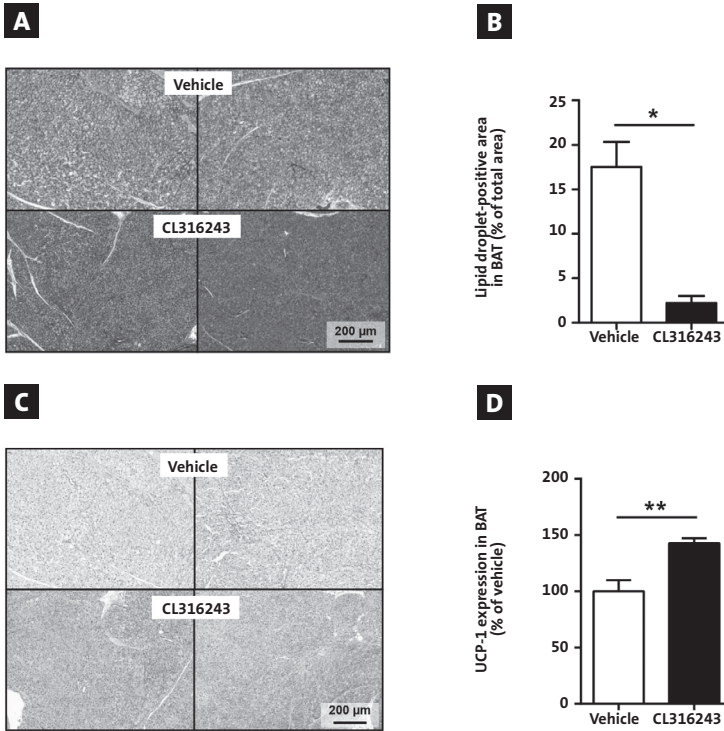


FIGURE S2 - β 3-AR agonism markedly increases brown adipose tissue activity. *E3L.CETP* mice were fed a Western-type diet and treated with vehicle or the β 3-AR agonist CL316243 during 10 weeks. Interscapular BAT was stained with HE and representative pictures are shown **A**. Lipid droplet-positive area was quantified using Image J software **B**. In addition, representative pictures are shown of UCP1-stained interscapular BAT **C**. The UCP1 expression was quantified using Image J software **D**.

Values are means \pm S.E.M. (panel B: n=3 per group; panel D: n=7-8 per group). * $P < 0.05$, ** $P < 0.01$.

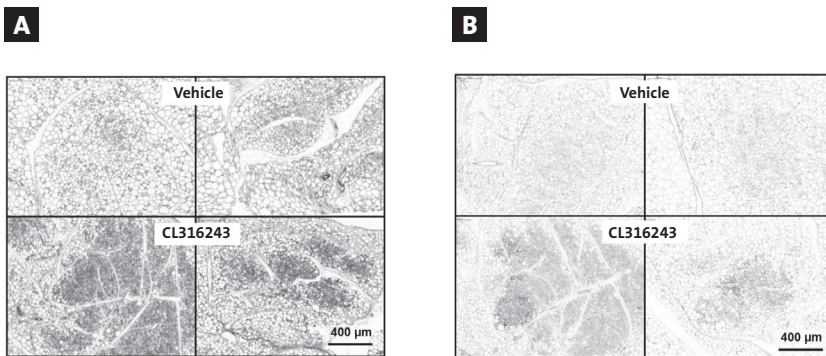


FIGURE S3 - β 3-AR agonism increases browning of white adipose tissue. *E3L.CETP* mice were fed a Western-type diet and treated with vehicle or the β 3-AR agonist CL316243 for 10 weeks. Epididymal WAT was stained with HE **A** and for UCP1 **B**, and representative pictures are shown.

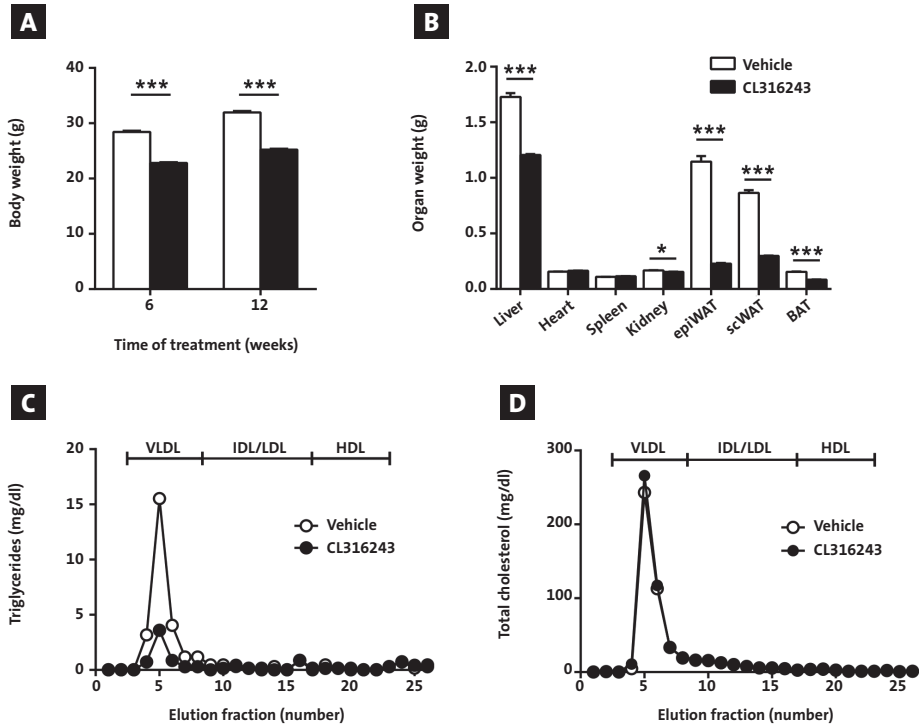


FIGURE S4 - BAT activation in *Apoe*^{-/-} mice reduces fat mass and plasma triglycerides, but not total cholesterol.

Apoe^{-/-} mice were fed a Western-type diet and treated with vehicle or the β_3 -AR agonist CL316243, pair-fed to the vehicle-treated group, during 12 weeks. Body weight was determined after 6 and 12 weeks of treatment **A**. Organ weight was determined after sacrifice at week 12 **B**. The distribution of triglycerides **C** and cholesterol **D** over lipoproteins was determined at week 12 in fasted plasma samples that were pooled per group. Values are means \pm S.E.M. (n=9-10 per group). * $P < 0.05$, *** $P < 0.001$.

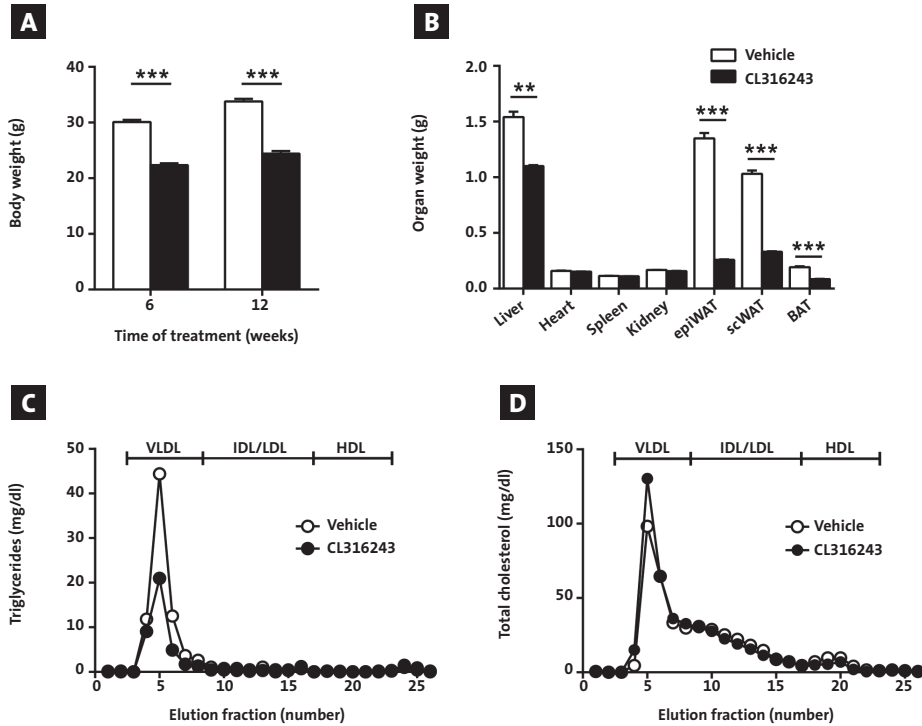


FIGURE S5 – BAT activation in *Ldlr*^{-/-} mice reduces fat mass and plasma triglycerides, but not total cholesterol. *Ldlr*^{-/-} mice were fed a Western-type diet and treated with vehicle or the β_3 -AR agonist CL316243, pair-fed to the vehicle-treated group, during 12 weeks. Body weight was determined after 6 and 12 weeks of treatment **A**. Organ weight was determined after sacrifice at week 12 **B**. The distribution of triglycerides **C** and cholesterol **D** over lipoproteins was determined at week 12 in fasted plasma samples that were pooled per group. Values are means \pm S.E.M. (n=8-11 per group). ** $P < 0.01$, *** $P < 0.001$.